Transition Metal Fischer-Type Complexes. Density Functional Analysis of the Systems $(CO)_5Cr{=}EH_2$ (E = C, Si, Ge, Sn) and $(CO)_5M{=}CH_2$ (M = Mo, W, Mn^+)

Heiko Jacobsen and Tom Ziegler*

Department of Chemistry, University of Calgary, 2500 University Drive N.W., Calgary, Alberta, Canada T2N 1N4

Received August 25, 1994[⊗]

The electronic and molecular structures of the title compounds have been investigated using density functional theory within the local density approximation, adding nonlocal corrections to exchange and correlation energy as a perturbation. The transition metal main group double bond was analyzed in terms of σ and π bond contributions. The main difference between chromium pentacarbonyl complexes with the carbene fragment compared to their higher homologues is a significant drop in the intrinsic π bond strength: $D_{\pi,\mathrm{int}}$(M═C) = 202 kJ/mol, $D_{\pi,\mathrm{int}}$ (M═Si) = 82 kJ/mol, $D_{\pi,\mathrm{int}}$ (M═Ge) = 72 kJ/mol, and $D_{\pi,\mathrm{int}}$ (M═Sn) = 51 kJ/mol. For the carbene complexes with transition metals of the chromium triad, the intrinsic π bond strengths are very similar: $D_{\pi,\mathrm{int}}$ (Cr═C) = 202 kJ/mol, $D_{\pi,\mathrm{int}}$ (Cr═Mo) = 204 kJ/mol, and $D_{\pi,\mathrm{int}}$ (Cr═W) = 221 kJ/mol. Relativistic effects are responsible for the increased π bond strength in the tungsten complex. The bond strengths for the metal carbon double bond rank as BE(W═C) > BE(Cr═C) > BE(Mo═C). Molecular orbital arguments are provided to explain the calculated trends. Further, the question of the rotational barriers around the M═E bond is addressed, and the differences in the geometry for the eclipsed as well as for the staggered conformation of $(CO)_5M{=}EH_2$ are analyzed.

1. Introduction

One of the most remarkable properties of transition metals is their ability to stabilize reactive and short-lived molecules. Classical examples are the transition metal carbene complexes,[1] which contain ligands bound through a disubstituted carbon atom. These compounds are generally divided into two classes. "Fischer-type"[2] carbenes are characterized by low-valent transition metals and an electrophilic carbene carbon. In contrast, the "Schrock-type"[3] compounds are formed with high-valent transition metals and posses a nucleophilic carbene carbon.

Soon after the discovery of the Fischer-type complexes[4] their benefit for organic synthesis has been realized and systematically explored. Most valuable are reactions in which the metal carbene complex serve as a C_1 synthon, as for example in inter-[5] and intramolecular[6] cyclopropanation reactions. In general, these complexes are utilized in a variety of reactions and now offer a broad potential for use in organic chemistry.[7,8]

Among the higher homologues of metal carbene complexes, a larger number of germylene, stannylene and even plumbylene systems have been structurally characterized.[9] According to Petz,[9] these complexes can roughly be divided into type I and type II class compounds. Compared to the type I complexes, which resemble the classical Fischer-type molecules, type II compounds show additional coordination of a Lewis base molecule B to the group XIV member E.

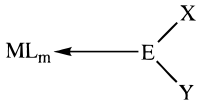

I

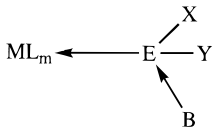

II

The first cationic[10] and neutral[11] type II coordination compounds of silylenes were reported in 1987. In the following years, Zybill and co-workers prepared a broad variety of Lewis stabilized silylene complexes[12] with the low valent transition metal fragments $Fe(CO)_4$ and $Cr(CO)_5$. The complexes of germylene and higher homologues usually contain low valent transition metals also, typically transition metal carbonyl fragments. In this respect all these molecules might be described as "Fischer-type like" complexes.

Whereas the area of structural chemistry of the higher homologues of Fischer-type carbenes is well developed, the investigations of the reactivity of these molecules are still in an early stage of development.[9,13] Consequently, only a few reactions involving silylene, germylene, and stannylene complexes are known in the literature, in sharp contrast to the richness of transition metal carbene chemistry.

Naked transition metal carbenes $M{=}CH_2$ have been carefully analyzed in a variety of theoretical studies.[14] They are of interest in their own right and serve as simple models for more complex compounds with a double bond between a transition metal and a group XIV element. Furthermore, neutral and cationic bare metal carbenes are experimentally accessible, and the dissociation energies for the metal−carbon double bonds are known for a variety of transition metals.[15,16] Cundari and Gordon[17]

[⊗] Abstract published in *Advance ACS Abstracts*, January 1, 1996.

(1) Dötz, K. H.; Fischer, H.; Hofmann, P.; Kreissl, F. R.; Schubert, U.; Weiss, K. *Transition Metal Carbene Complexes*; Verlag Chemie: Weinheim, Germany, 1983.
(2) Fischer, E. O. *Angew. Chem.* **1974**, *86*, 651.
(3) Schrock, R. R. *Acc. Chem. Res.* **1979**, *12*, 98.
(4) Fischer, E. O.; Maasböl, A. *Angew. Chem., Int. Ed. Engl.* **1964**, *3*, 580.
(5) Brookhart, M.; Studabaker, W. B. *Chem. Rev.* **1987**, *87*, 411.
(6) Söderberg, B. S.; Hegedus, L. S. *Organometallics* **1990**, *9*, 3113.
(7) (a) Dötz, K. H. *Pure Appl. Chem.* **1983**, *55*, 1689. (b) Dötz, K. H. *Angew. Chem., Int. Ed. Engl.* **1984**, *23*, 587.
(8) Hegedus, L. S. *Pure Appl. Chem.* **1990**, *62*, 691.
(9) Petz, W. *Chem. Rev.* **1986**, *86*, 1019.
(10) Straus, D. A.; Tilley, T. D.; Rheingold, A. L.; Geib, S. J. *J. Am. Chem. Soc.* **1987**, *109*, 5872.
(11) Zybill, C.; Müller, G. *Angew. Chem., Int. Ed. Engl.* **1987**, *26*, 669.
(12) (a) Zybill, C.; Müller, G. *Organometallics* **1988**, *7*, 1368. (b) Leis, C.; Wilkinson, D. L.; Handwerker, H.; Zybill, C.; Müller, G. *Organometallics* **1992**, *11*, 514. (c) Handwerker, H.; Paul, M.; Riede, J.; Zybill, C. *J. Organomet. Chem.* **1993**, *459*, 151.
(13) Zybill, C. *Top. Curr. Chem.* **1991**, *160*, 1.

0020-1669/96/1335-0775$12.00/0

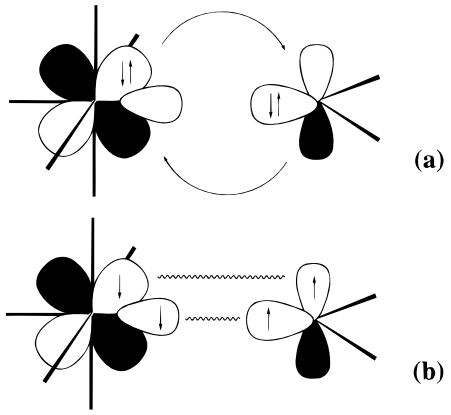

Figure 1. Possible bond descriptions for the M═E double bond in transition metal Fischer type complexes $(CO)_5M{=}EH_2$ (adapted from ref 20): (a) dative σ donor and π acceptor bonding between two singlet fragments. (b) covalent σ and π coupling between two triplet fragments.

have extended the theoretical work on bare metal carbenes to the transition-metal silicon double bond, and Márquez and Fernández Sanz[18] have presented a detailed CASSCF study on naked molybdenum complexes, including carbene, silylene, germylene, and stannylene ligands.

Calculations on carbene complexes in which the transition metal possesses a full coordination sphere are rather scarce. The first calculation on an *ab initio* level of theory for a transition metal carbonyl complex was reported by Spangler[19] and co-workers, who have chosen $(CO)_3NiCH_2$ as model for a Fischer-type complex. This model was later criticized by Hall and Taylor.[20] Using *ab initio* calculations with limited electron correlation, they differentiate between the electronic structures of Fischer-type and Schrock-type compounds. Fischer-type carbenes are formed by coordination of a singlet carbene ligand to a singlet transition metal fragment, resulting in a dative carbon to metal σ-donor bond and in a dative metal to carbon π bond (Figure 1a). In contrast, a Schrock-type complex results from the singlet coupling of a triplet carbene ligand to a triplet transition metal moiety, leading to nearly covalent σ and π bonds (Figure 1b).[20] From this point of view, CH_2 might not be a suitable ligand to model of Fischer-type complex, since its electronic ground state[21] is the triplet $^3B_1$. Thus, the carbene ligand for Fischer-type complexes is often modeled by CH(OH) with a singlet ground state, whereas the carbene ligand for Schrock-type compounds can be represented by CH_2. This was first done in the early studies on Fischer[22a] and Schrock[22b] type carbenes by Nakatsuji and co-workers. The authors provide the first optimized bond lengths, bond dissociation energies, and rotational barriers for the metal−carbon bonds in carbene complexes with the carbonyl fragment $Cr(CO)_5$ and $Fe(CO)_4$.[22a]

Only a few theoretical studies have been performed on the higher group XIV analogues of Fischer type complexes. The question as to whether a silylene−metal complex exists was brought forwarded by Nakatsuji and co-workers[23] in 1983. In an *ab initio* study, the authors calculated the metal−silicon bond in $Cr(CO)_5SiH(OH)$ to be about 63 kJ/mol weaker than in the corresponding carbene complex, demonstrating the possible existence of compounds with metal−silicon double bonds. They also reported that silylene complexes seem to be more reactive toward a nucleophilic attack than their carbene counterparts. To our knowledge, this investigation was the only one in its field for almost 10 years. The studies by Cundari and Gordon[17] on $M{=}SiH_2^+$ complexes (M = first row transition metal), including $Cr{=}GeH_2^+$ and $Cr{=}SnH_2^+$, and the work by Márquez and Fernández Sanz[18] on $Mo{=}EH_2$ systems (E = C, Si, Ge, Sn) initialized the theoretical work on naked transition metal complexes with higher group XIV ligands. In a series of papers, Cundari and Gordon[24] further analyzed the nature of the metal−carbon double bond in high valent transition metal alkylidene complexes or Schrock-type compounds, and they also expanded their studies to the hypothetical silylene analogues.[25] Márquez and Fernández Sanz[26] extended the thorough investigation of bare metal $Mo{=}EH_2$ systems with an *ab initio* CASSCF study of the $(CO)_5Mo{=}EH_2$ (E = C, Si, Ge, Sn) complexes.

Considering the importance of Fischer type carbenes as well as the recent developments in the field of silylene chemistry, it seems worthwhile to subject this class of compounds to a density functional study. Over the last decade, approximate density function theory (DFT) has evolved into a powerful tool for practical applications to molecular structures and energetics.[27] Furthermore, the use of the generalized transition state method not only provides accurate calculations of total bonding energies[28] but also allows for a breakdown of the bonding energy into steric as well as electronic contributions.[29] In this study, we investigate the influence of the variation of the group XIV member on the nature of the transition metal main group double bond. We hope to provide answers to the question of coordination chemistry and reactivity of the heavier analogues of carbene complexes. We further discuss the properties of carbene complexes with transition metal carbonyl fragments of the complete chromium triad. Calculations on $(CO)_5Mn{=}CH_2^+$ are also included, since for this molecule the M═C bond strength has been experimentally determined.

2. Computational Details

All calculations were performed utilizing the AMOL program package, developed by Baerends[30] et al. and vectorized by Ravenek.[31]

(14) (a) Brooks, B., Schaefer, H. F., III. *J. Mol. Phys.* **1977**, *34*, 193. (b) Goddard, W. A., III; Rappé, A. K. *J. Am. Chem. Soc.* **1977**, *99*, 3966. (c) Vincent, M. A.; Yoshioka, Y.; Schaefer, H. F., III. *J. Phys. Chem.* **1982**, *86*, 3905. (d) Carter, E. A.; Goddard, W. A., III. *J. Phys. Chem.* **1984**, *88*, 1485. (e) Carter, E. A.; Goddard, W. A., III. *J. Am. Chem. Soc.* **1986**, *108*, 2180. (f) Carter, E. A.; Goddard, W. A., III. *Organometallics* **1988**, *7*, 675. (g) Alvarado-Swaisgood, A. E.; Harrison, J. F. *J. Phys. Chem.* **1982**, *92*, 2757. (h) Planelles, J.; Merchán, M.; Tomás, F. *Chem. Phys. Lett.* **1988**, *149*, 222. (i) Mochizuki, T.; Tanaka, K.; Ohno, K.; Tatewaki, H.; Yamamoto, S. *Chem. Phys. Lett.* **1988**, *152*, 457. (j) Planelles, J.; Merchán, M.; Nebot Gil, I.; Tomás, F. *J. Phys. Chem.* **1989**, *93*, 6596. (k) Bauschlicher, C. W., Jr.; Partridge, H.; Sheehy, J. A.; Langhoff, S. R.; Rosi, M. *J. Phys. Chem.* **1992**, *96*, 6969.
(15) Armentrout, P. B.; Sunderlin, L. S.; Fisher, E. R. *Inorg. Chem.* **1989**, *28*, 4437.
(16) Martinho Simões, J. A.; Beauchamp, J. L. *Chem. Rev.* **1990**, *90*, 629.
(17) Cundari, T. R.; Gordon, M. S. *J. Chem. Phys.* **1992**, *96*, 631.
(18) Márquez, A.; Fernández Sanz, J. *J. Am. Chem. Soc.* **1992**, *114*, 10019.
(19) Spangler, D.; Wendoloski, J. J.; Dupuis, M.; Chen, M. M. L.; Schaefer, H. F., III. *J. Am. Chem. Soc.* **1981**, *103*, 3985.
(20) Taylor, T. E.; Hall, M. B. *J. Am. Chem. Soc.* **1984**, *106*, 1576.
(21) McKellar, A. R. W.; Bunker, P. R.; Sears, T. J.; Evenson, K. M.; Saykally, R. J.; Langhoff, S. R. *J. Chem. Phys.* **1983**, *79*, 5251.
(22) (a) Nakatsuji, H.; Ushio, J.; Han, S.; Yonezawa, T. *J. Am. Chem. Soc.* **1983**, *105*, 426. (b) Ushio, J.; Nakatasuji, H.; Yonezawa, T. *J. Am. Chem. Soc.* **1984**, *106*, 5892.
(23) Nakatsuji, H.; Ushio, J.; Yonezawa, T. *J. Organomet. Chem.* **1983**, *258*, C1.
(24) (a) Cundari, T. A.; Gordon, M. S. *J. Am. Chem. Soc.* **1991**, *113*, 5231. (b) Cundari, T. A.; Gordon, M. S. *J. Am. Chem. Soc.* **1992**, *114*, 539. (c) Cundari, T. A.; Gordon, M. S. *Organometallics* **1992**, *11*, 55.
(25) Cundari, T. A.; Gordon, M. S. *Organometallics* **1992**, *11*, 3123.
(26) Márquez, A.; Fernández Sanz, J. *J. Am. Chem. Soc.* **1992**, *114*, 2903.
(27) (a) Ziegler, T. *Pure Appl. Chem.* **1991**, *28*, 1271. (b) Ziegler, T. *Chem. Rev.* **1991**, *91*, 651. (c) *Density Functional Methods in Chemistry*; Labanowski, J., Andzelm, J., Eds.; Springer Verlag: Heidelberg, Germany, 1991.
(28) (a) Ziegler, T.; Rauk, A.; Baerends, E. J. *Theor. Chem. Acta* **1977**, *43*, 261. (b) Ziegler, T.; Rauk, A. *Theor. Chim. Acta* **1977**, *46*, 1.
(29) (a) Baerends, E. J.; Rozendaal, N. *NATO ASI Sec. C* **1986**, *C176*, 159. (b) Ziegler, T. *NATO ASI Sec. C* **1991**, *C378*, 367.

The numercial integration was performed according to the procedure developed by teVelde[32] et al. The exchange factor, α_{ex}, was given the usual value of $^2/_3$. Electron correlation was treated within the Local Density Approximation (LDA) in the parametrization of Vosko[33] et al. The final energies were determined by adding Becke's[34] nonlocal exchange correction as well as Perdew's[35] inhomogeneous gradient corrections for correlation (LDA/NL) as a perturbation. An uncontracted triple ζ-STO basis set[36] was used for the *n*s, *n*p, *n*d, $(n + 1)$s, and $(n + 1)$p shells of the transition metals. For H, a double ζ-STO basis set[36] was employed, which was extended by one 2p-STO polarization function. The *n*s and *n*p shells of the remaining main group elements were described by a double ζ-STO basis set,[36] augmented by one 3d-STO polarization function for C and O and by one *n*d-STO polarization function for Si, Ge, and Sn. Electrons in lower shells were considered as core and treated according to the procedure of Baerends[30] et al. An auxiliary set[37] of s, p, d, f, and g STO functions, centered on all nuclei, was used in order to fit the molecular density and present Coulomb and exchange potentials accurately in each SCF cycle. The geometry optimization procedure was based on the method of Versluis and Ziegler.[38] All geometries were optimized at the LDA level of theory and without explicit treatment of relativistic effects. For the tungsten system, the final electronic structure and bonding energy was calculated by taking relativistic corrections into account according to the scheme devised by Snijders[39] and co-workers.

3. Results and Discussion

We optimized the molecular structures for the following $(CO)_5Cr{=}EH_2$ systems: E = C (**Ia**), Si (**IIa**), Ge (**IIIa**), and Sn (**IVa**). In addition, we performed calculations on $(CO)_5Mo{=}CH_2$ (**Ib**), $(CO)_5W{=}CH_2$ (**Ic**), and $(CO)_5Mn{=}CH_2^+$ (**Id**). Before we begin with the detailed discussion of our results, we will present a brief outline of our energy decomposition scheme.

Methodology of the Bonding Analysis. We analyze the bonding in $(CO)_5M{=}EH_2$ by looking at the interaction of the metal pentacarbonyl fragment with the EH_2 moiety. The total bond energy BE than can be written as[29]

$$\mathrm{BE} = -[\Delta E^0 + \Delta E_{\mathrm{int}} + \Delta E_{\mathrm{prep}}] \qquad (1)$$

with ΔE^0 as the steric repulsion, ΔE_{int} as the orbital interaction energy and ΔE_{prep} as the preparation energy. The term ΔE^0 consists of two components:

$$\Delta E^0 = \Delta E_{\mathrm{elstat}} + \Delta E_{\mathrm{Pauli}} \qquad (1a)$$

Here, $\Delta E_{\mathrm{elstat}}$ describes the pure Coulomb interaction between the two fragments, and it is usually attractive. The term $\Delta E_{\mathrm{Pauli}}$, which is called exchange repulsion or Pauli repulsion, takes into account the destabilizing two-orbital three- or four-electron interactions between occupied orbitals on both fragments. We like to point out that our definition for the steric repulsion includes the Coulomb interaction term, whereas often the steric repulsion is understood as $\Delta E_{\mathrm{Pauli}}$ only. The second term on the right hand side of equation **1**, ΔE_{int}, includes the attractive orbital interaction between occupied and virtual orbital on the two fragments. ΔE_{int} can be analyzed in terms of orbital interactions from different irreducible representations.[29] This concept relates strongly to the idea of σ and π bond strengths. Thus, we break down ΔE_{int} according to

$$\Delta E_{\mathrm{int}} = -[D_{\sigma,\mathrm{int}} + D_{\pi,\mathrm{int}}] \qquad (1b)$$

where we define $D_{\sigma,\mathrm{int}}$ and $D_{\pi,\mathrm{int}}$ as our intrinsic σ and π bond strengths, respectively. Orbitals that have the plane defined by the EH_2 ligand as a nodal plane, contribute to $D_{\pi,\mathrm{int}}$. Similarly, orbitals that lie in the plane of the EH_2 ligand donate to $D_{\sigma,\mathrm{int}}$. The terms ΔE^0 and ΔE_{int} combine to the so called bond snapping energy $\mathrm{BE}_{\mathrm{snap}}$:

$$\mathrm{BE}_{\mathrm{snap}} = -[\Delta E^0 + \Delta E_{\mathrm{int}}] \qquad (1c)$$

The last term on the right hand side of equation **1**, ΔE_{prep}, takes into account the deformation energy of the fragments from their equilibrium geometries to the framework of the final molecule, $\Delta E^{\mathrm{g}}_{\mathrm{prep}}$, and, if required, the promotion energy from the electronic ground state of the fragments to their electronic valence configuration, $\Delta E^{\mathrm{e}}_{\mathrm{prep}}$. We shall write the preparation energy as

$$\Delta E_{\mathrm{prep}} = \Delta E^{\mathrm{g}}_{\mathrm{prep}} + \Delta E^{\mathrm{e}}_{\mathrm{prep}} \qquad (1d)$$

We refer the reader to the original literature[28,29] as well as to some recent applications[40,41] for a more detailed account of the method.

Next we have to define the electronic valence states for the bonding interaction. One might consider a coupling of two singlet fragments, as shown in Figure 1a, or, alternatively, the interaction of two triplet species, as in Figure 1b. The chromium pentacarbonyl fragment itself has a singlet ground state, and in cases where the group XIV fragment also possesses a singlet ground state, the dative interaction (Figure 1a) seems to be the natural choice.

The situation is different if we consider ligands which have a triplet state. To prepare the CH_2 moiety for a dative interaction, we have to excite the molecule into its singlet valence state. On the LDA/NL level of theory, we calculated $\Delta E^{\mathrm{e}}_{\mathrm{prep}}$ to be 65 kJ/mol.[41] On the other hand, we might promote the metal fragment to its triplet state, and describe the M═E bond as covalent σ and π bonds (Figure 1b). This step would require a $\Delta E^{\mathrm{e}}_{\mathrm{prep}}$ of 141 kJ/mol. From this comparison it is obvious that a dative interaction scheme between two singlet fragments should be favored since it gives the smallest $\Delta E^{\mathrm{e}}_{\mathrm{prep}}$ terms.

An exemplary bonding analysis for $(CO)_5Cr{=}CH_2$ is shown in Figure 2. It is noteworthy that the value for $\Delta E^{\mathrm{g}}_{\mathrm{prep}}$ is less than 5% of the bond snapping energy and does not significantly influence the total bonding energy. For the molecules with a heavier group XIV element, the ligand possesses a singlet ground state, and no electronic preparation is required. In this cases, the bond snapping energy $\mathrm{BE}_{\mathrm{snap}}$ is a reasonable approximation to the total bonding energy BE.

(30) (a) Baerends, E. J.; Ellis, D. E.; Ros, P. E. *Chem. Phys.* **1973**, *2*, 41. (b) Baerends, E. J. Ph.D. Thesis, Vrije Universiteit Amsterdam, 1975.
(31) Ravenek, W. In *Algorithms and Applications on Vector and Parallel Computers*; Riele, H. H. J., Dekker, Th. J., van de Horst, H. A., Eds.; Elsevier: Amsterdam, 1987.
(32) teVelde, G.; Baerends, E. J. *J. Comput. Phys.* **1992**, *99*, 84.
(33) Vosko, S. J.; Wilk, M.; Nusair, M. *Can. J. Phys.* **1980**, *58*, 1200.
(34) (a) Becke, A. *J. Chem. Phys.* **1986**, *84*, 4524. (b) Becke, A. *J. Chem. Phys.* **1988**, *88*, 1053.
(35) Perdew, J. P. *Phys. Rev.* **1986**, *B33*, 8822.
(36) (a) Snijders, G. J.; Baerends, E. J.; Vernoijs, P. *At. Nucl. Data Tables* **1982**, *26*, 483. (b) Vernooijs, P.; Snijders, G. J.; Baerends, E. J. *Slater Type Basis Functions for the Whole Periodic Table*; Internal Report; Vrije Universiteit Amsterdam: Amsterdam, 1981.
(37) Krijn, J.; Baerends, E. J. *Fitfunctions in the HFS-Method*; Internal Report; Vrije Universiteit Amsterdam: Amsterdam, 1984.
(38) Versluis, L.; Ziegler, T. *J. Chem. Phys.* **1988**, *88*, 322.
(39) (a) Snijders, J. G.; Baerends, E. J. *Mol. Phys.* **1978**, *36*, 1789. (b) Snijders, J. G.; Baerends, E. J.; Ros, P. *Mol. Phys.* **1979**, *38*, 1909. (c) Ziegler, T.; Tschinke, V.; Baerends, E. J.; Snijders, J. G.; Ravenek, W. *J. Phys. Chem.* **1989**, *93*, 3050.
(40) (a) Rosa, A.; Baerends, E. J. *New J. Chem.* **1991**, *15*, 815. (b) Rosa, A.; Baerends, E. J. *Inorg. Chem.* **1992**, *31*, 4717.
(41) Jacobsen, H.; Ziegler, T. *J. Am. Chem. Soc.* **1994**, *116*, 3667.

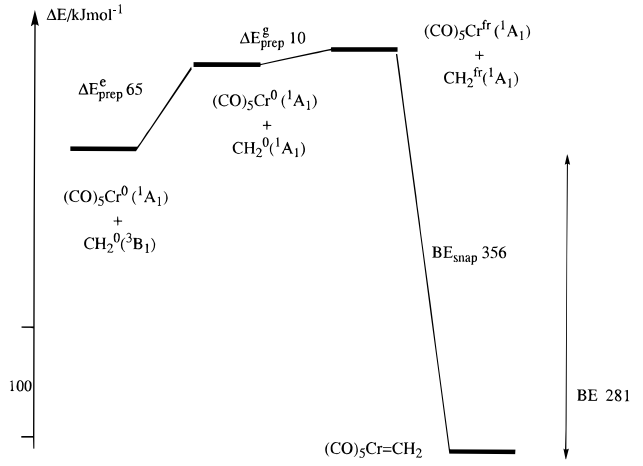

Figure 2. Schematic bond analysis for the $(CO)_5Cr{=}CH_2$ complex.

The question of Fischer type vs Schrock type complexation has also been discussed by Márquez and Fernández Sanz.[26] In case of the naked $Mo{=}EH_2$ complexes, the authors find a Schrock type complexation favored for all systems. This is in accordance with the results of Cundari and Gordon,[17] who reported that for the early and middle transition metals (Sc and Mn) the electronic structure of $M{=}SiH_2^+$ complexes is dominated by covalent resonance structures. However, Márquez and Fernández Sanz[26] analyzed the changes in the $Mo{=}EH_2$ bond lengths and bond strengths under carbonylation of the metal fragment. They conclude that for $(CO)_5Mo{=}EH_2$ compounds a Fischer-type description is more appropriate. This is especially true in the case of $(CO)_5Mo{=}CH_2$. The electronic ground state of the $(CO)_5M$ fragment rather than that of the EH_2 moiety dominates the character of the M=E double bond. Thus, even for methylene complexes a donor-acceptor bond description is most appropriate.

Structures and Bonding of $(CO)_5Cr{=}EH_2$ (E = C, Si, Ge, Sn). Considering the geometries of $(CO)_5M{=}EH_2$ complexes, we can in principal differentiate between two conformations of the EH_2 ligand, namely an eclipsed arrangement *E* as well as a staggered arrangement *S*. Further, one might consider a geo-

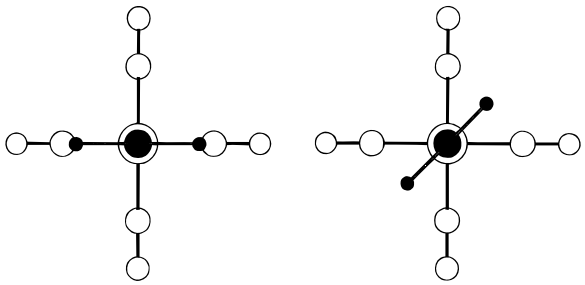

E ***S***

metric arrangement possessing a bent EH_2 moiety. These structural alternatives are realized for the heavier analogues of ethylene,[41] leading to trans−bent rather than planar $H_2E{=}EH_2$ molecules. However, in the case of the transition metal complexes investigated in this study, the appropriate virtual orbitals are too high in energy to favor a Jahn−Teller distortion toward a bent structure.

The experimentally known structures for Fisher type carbenes with chromium pentacarbonyl show that the carbene plane is roughly staggered with the *cis* carbonyl ligands. It has been argued[42] that this is mainly due to the sterically demanding

(42) Schubert, U. *Coord. Chem. Rev.* **1984**, *55*, 261.

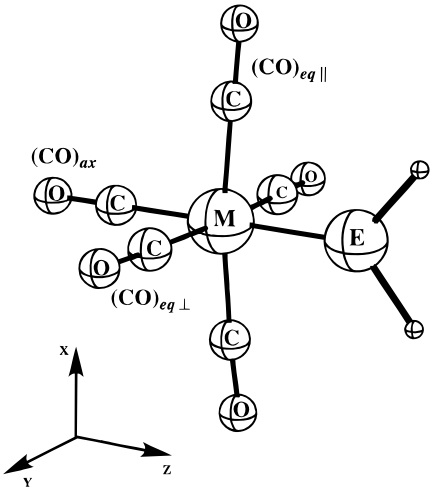

Figure 3. Eclipsed geometry of $(CO)_5M{=}EH_2$ complexes. Equatorial CO ligands are designated as $(CO)_{eq\perp}$ and $(CO)_{eq||}$, respectively.

Table 1. Optimized Bond Distances[a] and Bond Angles for $(CO)_5Cr{=}EH_2$ Complexes

	Ia: E = C	**IIa**: E = Si	**IIIa**: E = Ge	**IVa**: E = Sn
d(Cr−E)	188.4	220.1	227.9	243.0
d(E−H)	110.7	150.8	156.2	173.1
∠(HEH)	109.9	102.7	103.6	103.3
$d(Cr-C)_{ax}$	189.2	185.4	184.7	183.4
$d(Cr-C)_{eq\|\|}$	185.4	184.7	184.8	184.9
$d(Cr-C)_{eq\perp}$	187.6	186.0	186.0	186.1
$d(C-O)_{ax}$	114.6	114.5	114.8	114.8
$d(C-O)_{eq\|\|}$	115.0	115.2	115.1	115.2
$d(C-O)_{eq\perp}$	114.5	115.0	114.8	115.0
$\angle(H_2E-CrC_{eq\|\|})$	86.2	85.0	86.2	85.8
$\angle(H_2E-CrC_{eq\perp})$	91.7	92.1	92.1	92.0

[a] Distances in pm; angles in deg.

substituents of the carbene ligand. The studies of Nakatsuji[22a] and co-workers on $(CO)_5Cr{=}CH(OH)$, and of Márquez and Fernández Sanz[26] on $(CO)_5Mo{=}EH_2$ report barriers of 1−2 kJ/mol for a rotation around the M=E bond, favoring the eclipsed conformation to be more stable. The small barriers indicate that this rotation is essentially free. We will at a later point in our discussion return to the problem of rotational barriers.

Figure 3 diplays a representative eclipsed geometry for $(CO)_5M{=}EH_2$ systems. We can distinguish between two different groups of *cis* or equatorial carbonyls. CO ligands, which are perpendicular with respect to the plane of the carbene moiety, are denoted as $(CO)_{eq\perp}$. The other set of CO ligands is then called $(CO)_{eq||}$. The optimized geometries for complexes **Ia**, **IIa**, **IIIa** and **IVa** are collected in Table 1.

On going from the carbene to the stannylene complex, we note a steady increase in the M=E bond length. The most drastic change is observed between the CH_2 and the SiH_2 complex. Further, the lengthening of the M=E bond is accompanied by a decrease of the $M-C_{ax}$ distance. The geometry of $Cr(CO)_6$ has recently been reevaluated,[43] and the LDA value for the Cr−C bond length amounts to 186.6 pm. Whereas in the carbene compound **Ia** the $M-C_{ax}$ bond length is larger than for a Cr−C bond in $Cr(CO)_6$, we find for the higher analogues **IIa**, **IIIa**, and **IVa** that the $M-C_{ax}$ bond is shortened. The $(CO)_{eq||}$ ligand shows for all systems a relatively short M−C bond around 185 pm. This ligand does not compete with the EH_2 group for bonding orbitals of the metal center. In

(43) (a) Li, J.; Schreckenbach, G.; Ziegler, T. *J. Phys. Chem.* **1994**, *98*, 4838. (b) Li, J.; Schreckenbach, G.; Ziegler, T. *J. Am. Chem. Soc.* **1995**, *117*, 486.

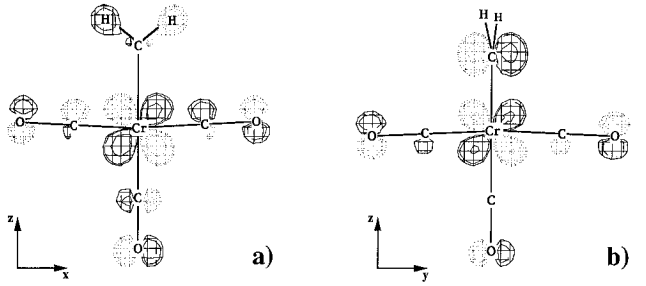

Figure 4. 3D contour plots of the (a) HOMO and (b) HOMO-2 of $(CO)_5Cr{=}CH_2$. The contour value chosen is 0.05 au.

contrast, the $(CO)_{eq\perp}$ shares the back-bonding donation of one of the metal d-orbitals with the EH_2 ligand. Consequently, this M−C bond length is slightly elongated. All C−O distances amount to about 115 pm and are 2 pm longer than for free CO (LDA, d_{C-O} = 113.1 pm; experiment, d_{C-O} = 112.83 pm[44]).

Another interesting structural aspect concerns the angles $\angle(ECrC)_{eq}$. The $(CO)_{eq||}$ groups are slightly bent toward the EH_2 ligand and form angles $\angle(ECrC)_{eq||}$, which are smaller than 90°. On the other hand, the angles $\angle(ECrC)_{eq\perp}$ are slightly larger than 90°, and $(CO)_{eq\perp}$ ligands are tilted away from the EH_2 group. In order to understand how this deformation might influence the electronic structure of the complexes, we will analyze the highest two occupied orbitals, which carry contributions form the EH_2 ligand. For complex **Ia**, 3D contour plots for the HOMO, $1b_1$, and for the HOMO-2, $1b_2$, are presented in parts a and b of Figure 4, respectively. The HOMO-1, $1a_2$, is made up of a combination of CO and Cr orbitals, only. The orbitals $1b_1$, $1a_2$ and $1b_2$ correspond to the three metal based d-type t_{2g} orbitals in an octahedral framework.

The CH_2 contribution to the HOMO, $1b_1$, is an occupied C-H bonding orbital, which undergoes a repulsive interaction with the metal $3d_{zx}$ orbital. In this irreducible representation, the carbene ligand does not possess any empty orbitals suitable for back donation from the metal fragment. On the other hand, the axial CO group has an empty π^* orbital, which can accept electron density from the Cr-$3d_{zx}$ orbital. The axial CO ligand competes with two of the equatorial CO groups, namely the $(CO)_{eq||}$, for back-bonding from the metal center. To compensate for the lack of π bonding with the carbene ligand, the $(CO)_{eq||}$ ligands bent slightly toward the CH_2 group, and so enhance the π bonding of the axial CO group with the metal center. Under this geometry distortion, the overlap of a $(CO)_{eq||}$ π^* orbital with the Cr-$3d_z$ *is* reduced. This now allows for a better interaction between $(CO)_{ax}$ and the metal center. We can understand this stabilization in the following way. We consider the electron donation from the $(CH_2)(CO)_4Cr$ fragment to the axial CO group. The geometry distortion will raise the occupied π fragment orbital of the metal center in energy and will bring it energetically closer to the acceptor orbital of the CO ligand. Therefore, the metal fragment and the axial CO group can undergo a stronger bonding interaction.

For the HOMO-2, $1b_2$, the situation is different. Here, the carbene ligand has an empty C-$2p_y$ orbital, which is available for back donation form the Cr-$3d_{zy}$ orbital. This orbital interaction is favored over the donation into the π^* orbital of the $(CO)_{ax}$ ligand. Thus, the $(CO)_{eq\perp}$ moieties are now bent away from the CH_2 group. We can understand the stabilizing effet of this distortion using the same reasoning as for the case of the HOMO, $1b_1$.

The effect discussed above is small, but noticeable. In a case study of the $Cr(CO)_5$ fragment, we found that a bending of two opposite $(CO)_{eq}$ ligands toward the $(CO)_{ax}$ ligand by 5° increases the energy of the HOMO from −6.438 eV up to −6.382 eV. The overlap of the C-2p fragment orbitals of the moving $(CO)_{eq}$ ligands with the Cr-3d orbital reduces from 0.2208 to 0.2149.

Another possible explanation for a distortion from an ideal octahedral or pseudooctahedral framework is based on the reduction of symmetry.[45] Orbital that were of different irreducible representations in higher symmetry might transform according to the same irreducible representation in lower symmetry, and thus they can intermix. For the HOMO, $1b_1$, we can think of a mixing between the occupied Cr-$3d_{zx}$ and the empty Cr-$4p_x$ orbital. The resulting pd hybrid, as shown in **1**, could be polarized toward the $(CO)_{ax}$ ligand and away from the CH_2 which lacks the ability of π bonding.

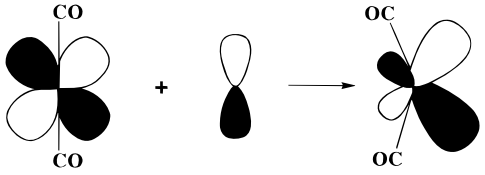

1

Nonetheless, in our particular case, bending of the $(CO)_{eq}$ ligands does not lead to a reduction of symmetry. During this process, C_{2v} symmetry is preserved. Any orbital mixing that is allowed for the bent geometries is therefore also allowed for geometric arrangements with angles $\angle(CO-Cr-CH_2) = 90°$. An analysis of the composition of the HOMO, $1b_1$, and the HOMO-2, $1b_2$, reveals that these MOs do not carry any contributions from Cr-$4p_x$ and Cr-$4p_y$ orbitals, respectively. The stabilization stems solely from the reduced bonding interaction of $(CO)_{eq}$ ligands with the metal center, which allows for a stronger bonding of the EH_2 group and the $(CO)_{ax}$ ligand.

We now turn to an analysis of the M=E bond strengths. The bonding energies BE and their decomposition are presented in Table 2. The values for BE as well as those for the bond snapping energy BE_{snap} decrease with increasing atomic number of E. Since the CH_2 fragment possesses a triplet ground state, we have to promote it to its singlet valence state. The other EH_2 fragments have a singlet ground state and therefore do only require a geometric preparation. As a consequence, the prepara-

Table 2. Bond Analysis[a] for $(CO)_5Cr{=}EH_2$ Complexes[a]

	ΔE^0	ΔE_{int}	$D_{\sigma,int}$	$D_{\pi,int}$	BF_{snap}	ΔE_{prep}	BE
Ia: E = C	113	−469	267	202	356	75	281
IIa: E = Si	157	−414	332	82	257	16	241
IIIa: E = Ge	134	−340	268	72	206	20	186
IVa: E = Sn	150	−334	283	51	184	21	163

[a] Energies are evaluated at the LDA/NL theory, and are in kJ/mol.

Table 3. Mulliken Population Analysis for the M=E Double Bonds in $(CO)_5Cr{=}EH_2$[a]

	σ(E→Cr)		π(Cr→E)	
	$Q(Cr(CO_5))$	$Q(EH_2)$	$Q(Cr(CO_5))$	$Q(EH_2)$
Ia: E = C	0.583	1.324	1.406	0.625
IIa: E = Si	0.828	1.117	1.682	0.311
IIIa: E = Ge	0.743	1.198	1.690	0.304
IVa: E = Sn	0.749	1.250	1.743	0.254

[a] Fragment populations for the σ component (donation from the ligand to the metal fragment) and for the π component (back donation from the metal fragment to the ligand) of the M=E bond are presented.

(44) *CRC Handbook of Chemistry and Physics*, 74th ed.; Lide, R. D., Ed.; CRC Press: Boca Raton, FL, 1993; p **9**-15.

(45) (a) Albright, T. A.; Brudett, J. K.; Wanghbo, M. H. *Orbital Interactions in Chemistry* John Wiley: New York, 1985. (b) Versluis, L. Ph.D. Thesis, University of Calgary, 1989.

Table 4. Bonding Analysis[a] for the Eclipsed *E* and Staggered *S* Conformations of $(CO)_5Cr{=}CH_2$, **Ia**, and $(CO)_5Cr{=}SiH_2$, **IIa**

	ΔE_{prep}	ΔE^0	ΔE_{int}	BE_{snap}	BE
$(CO)_5Cr{=}CH_2$, *E*	74.7	113.1	−469.3	356.2	281.5
$(CO)_5Cr{=}CH_2$, *S*	75.6	113.3	−470.8	357.6	282.0
$(CO)_5Cr{=}SiH_2$, *E*	16.2	157.1	−414.4	257.3	241.1
$(CO)_5Cr{=}SiH_2$, *S*	15.6	158.1	−414.3	256.2	240.6

[a] Energies in kJ/mol.

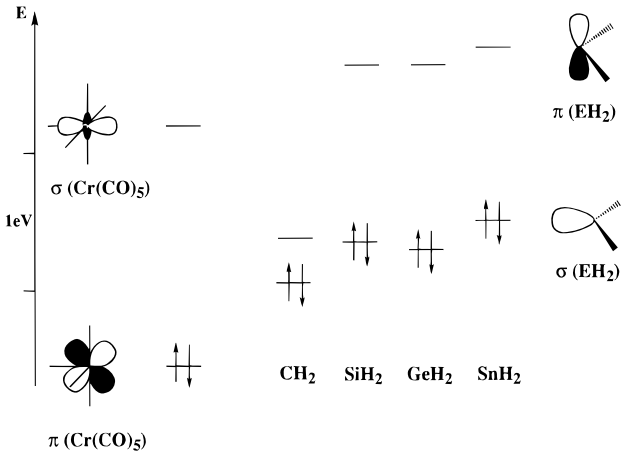

Figure 5. Frontier orbital diagram for the valence configuration of the $(CO)_5Cr$ fragment and of the EH_2 ligands.

tion energy for **Ia** is with 75 kJ/mol about four times higher than for the complexes **IIa**, **IIIa**, and **IVa**. Thus, the Cr=C bond is only 40 kJ/mol more stable than the Cr=Si bond. The values for the Cr=Si and the Cr=Ge bonds are comparable with calculated[41] Si=Si and Ge=Ge double bond strengths, respectively. For tin, we find that the Sn=Cr bond is roughly 40 kJ/mol more stable than the Sn=Sn double bond.[41]

The trend observed for the bond energies is clearly reflected in the orbital interaction energy. Of special interest are the changes in the π-component of ΔE_{int}. The carbene complex has an intrinsic π-bond strength of 202 kJ/mol. This value drops to 92 kJ/mol for the silylene complex and successively decreases to 72 kJ/mol for **IIIa** and 51 kJ/mol for **IVa**. We note that the π-bond for the heavier carbene analogues is fairly weak. A popular reasoning for the decrease in π-bond strength makes use of the increasing diffuse nature of the p_π(E) orbital, leading to less effective overlap with the d_π(Cr) orbital. However, if we analyze the values of the p_π(E)−d_π(Cr) overlap integrals, we find a rather steady decrease which does not explain the drastic change in $D_{\pi,int}$ between carbon and its higher homologues: $S_{p(C),d(Cr)} = 0.181$, $S_{p(Si),d(Cr)} = 0.173$, $S_{p(Ge),d(Cr)} = 0.163$, and $S_{p(Sn),d(Cr)} = 0.151$. A better explanation for the difference in π bond strength can be found by looking at the match in energy of the interacting fragment orbitals. In Figure 5, the relative energies for the σ- and π-type frontier orbitals of the $Cr(CO)_5$ and EH_2 fragments are displayed. We note that the empty $\pi(EH_2)$ orbitals for E = Si, Ge, and Sn are about 1.3 eV higher in energy than the $\pi(CH_2)$ orbital. Consequently, the $\pi(CH_2)$ orbital is energetically much better suited for accepting electron density from the donating $\pi(Cr(CO)_5)$ orbital than is any of the π-type orbitals of the higher homologues.

Due to an extended electronic core, the atomic nucleus is more effectively shielded for Si, Ge, and Sn than it is for C. This is represented in the Mulliken atomic chages AC at E in $(CO)_5Cr{=}EH_2$ complexes: AC(C) = −0.440, AC(Si) = 0.561, AC(Ge) = 0.612, and AC(Sn) = 0.570. We see that another important difference between **Ia** and its higher homologues is that, only for the carbene complex, the E atom carries a negative charge, whereas for all other cases the charge on E is positive.

The changes in π bond strength can further be seen in the different trans-effect of complexes **Ia** to **IVa**. As we pointed out earlier, only complex **Ia** shows a slightly elongated M−C_{ax} bond distance, indicating that the CH_2 ligand competes with the *trans* CO for π acceptance. For the heavier homologues, M−C_{ax} is shortened, and in these complexes the *trans* CO ligand can undergo a more efficient back bonding interaction.

The basic trend in the steric interaction and in the σ component $D_{\sigma,int}$ is an increase in both ΔE^0 as well as in $D_{\sigma,int}$. Our analysis suggests that silylene, germylene, and stannylene are in general better σ donors than carbene, with silylene being the most efficient one. In any case, on going from **Ia** to **IVa**, we note that there is a fluctuation in the relative changes in ΔE^0 and $D_{\sigma,int}$. We will therefore evaluate those terms together, and to this end we introduce the reduced intrinsic σ bond strength $D'_{\sigma,int}$:

$$D'_{\sigma,int} = D_{\sigma,int} - \Delta E^0 \qquad (2)$$

This definition can be justified by noting that the σ donation from the double-occupied p_π(E) orbital not only provides the major contribution to the orbital interaction energy, but also to the intermolecular steric interaction. In a sense, this orbital comes closest to the occupied orbitals at the metal center. We calculate the following values for $D'_{\sigma,int}$: **Ia**, 154 kJ/mol; **IIa**, 175 kJ/mol; **IIIa**, 134 kJ/mol; **IVa**, 133 kJ/mol. Also in terms of $D'_{\sigma,int}$, the silylene ligands prove to be the best σ donor. The reduced σ donor strength for germylene and stannylene are about the same, being 20 kJ/mol less than the value for carbene. One important factor, which makes SiH_2 a better σ donor than CH_2, can be found in the difference in spatial extend of the valence p orbitals. Since the electronic core of the C atom only consists of s orbitals, its 2s and 2p valence orbitals are localized in roughly the same region of space.[46] This leads not only to short M=C bonds but also to an enhanced steric repulsion between s core orbitals of the C atom and the transition metal. In contrast, the 3p orbital of Si is of greater extent in space, due to p orbitals in the electronic core. Therefore, the 3p(Si) orbital has a better overlap with the 3d(Cr) orbital than the 2p(C) orbital, $S^\sigma_{p(Si),d(Cr)} = 0.391$ compared to $S^\sigma_{p(C),d(Cr)} = 0.354$, leading to a stronger M=E bond. The $S^\sigma_{p(C),d(Cr)}$ overlap could be improved by a further shortening of the M=C bond, but the gain in orbital interaction cannot pay the price of an enhanced steric repulsion. On going to Ge and Sn, we now have additional steric repulsion between d orbitals in the electronic core of the main group element and the valence d orbitals of the transition metal. This leads to further elongation of the M=E distance and to a decrease in the reduced σ donor strength.

Finally, we will discuss the M=E double bond in terms of a Mullikan population analysis. For the σ- as well as for the π-bonding orbitals, Mulliken populations on the two fragments are presented in Table 3. In some cases, the fragment occupations do not add up to the total molecular orbital occupation. For those molecules, we have additional small contributions of higher, unoccupied fragment orbitals to σ- and π-bonding, respectively. Similarly, if one of the fragments additionally contributes to other bonding orbitals, the total sum of the fragment populations will be slightly larger than the total molecular orbital occupation. The σ bond charges at the $Cr(CO)_5$ fragment of complexes **Ia** to **IVa** again indicate that SiH_2 should be the strongest σ donor, and that GeH_2 and SnH_2 should have an equivalent σ donor strength. The fact that the last two ligands possess smaller $D'_{\sigma,int}$ values than carbene can be explained with the contribution of the steric interaction ΔE^0

(46) Kutzelnigg, W. *Angew. Chem., Int. Ed. Engl.* **1984**, *23*, 272.

to the reduced intrinsic σ bond strength. The π bond charges show the relative significance of back-bonding for the complexes **Ia** to **IVa**. They resemble the trend observed for the values of $D_{\pi,\text{int}}$. The value of Q(EH_2) roughly drops by a factor of two, when going from the carbene to the silylene complexes and decreases less drastically for complexes **IIIa** and **IVa**.

We summarize the bond analysis by correlating our results with the known chemistry of silylene, germylene, and stannylene compounds. In view of the weak π-bond strength, it is not surprising that these species follow a tendency to form Lewis base adducts and to undergo type II complexation. The ligand association energy will in most cases be favored over the additional π bonding with the metal fragment. The fact that these compounds act as Lewis acids can further be understood considering the positive partial charge at the E center. Common reactions for the type II compounds are replacement reactions at the ER_2 ligands. Those might be classified as S_N2 type processes, which in turn represent the most common modifications of a fully saturated carbon center.

We now return to the question of rotational barriers. We optimized staggered geometries for the carbene complex, **Ia**, as well as for the silylene complex **IIa**. A notable change in the geometry is a small decrease of the Cr−E distance (d_{Cr-CH_2} = 187.8pm, d_{Cr-SiH_2} = 219.5 pm). Further, all $(CO)_{eq}$ ligands are now bent toward the EH_2 group and form angles, $\angle(EH_2-Cr-C)_{eq}$, which are smaller than 90° ($\angle(CH_2-Cr-C)_{eq}$ = 89.2°, $\angle(SiH_2-Cr-C)_{eq}$ = 88.3°). This "umbrella effect" is often found in experimental structures,[47] and it has been explained on the basis of solid state packing.[48] However, we can understand this geometric distortion by following the same reasoning as used for the eclipsed geometries. If the carbene or silylene ligand is rotated by 45°, all equatorial CO groups become equivalent. We therefore expect that now the $(CO)_{eq}$ groups are bent either toward the CH_2 or toward the axial CO ligand. This motion would then stabilize the HOMO or the HOMO-2, respectively. According to the frontier orbital principle, the HOMO dominates the electronic structure of the complex. The $(CO)_{eq}$ ligands will bent toward the side of the EH_2 group and thus stabilize the $(CO)_{ax}$-based HOMO of the complex.

In contrast to the results of Nakatsuji[22a] and co-workers and to that of Márquez and Fernández Sanz,[26] we find that for the carbene complex **Ia** the staggered geometry is favored by 0.5 kJ/mol. The bond analysis for both configurations is presented in Table 4. We see that both the steric repulsion as well as the orbital interaction increases, when **Ia** is rotated from an eclipsed into a staggered geometry. Two factors are responsible for the change in ΔE^0. In the staggered conformation, the substituents of the ER_2 ligand suffer less steric repulsion from the $(CO)_{eq}$ ligands. On the other side, since now all $(CO)_{eq}$ ligands are bent toward the EH_2 group, the steric interaction between the EH_2 ligand and the $(CO)_{eq}$ group increases. For the term ΔE_{int}, we have a reduction in π back-bonding to the EH_2 ligand, which in turn is accompanied by an enhanced interaction of the $(CO)_{ax}$ ligand with the metal center. The values presented in Table 4 show that there exists a subtle balance between the effects mentioned above. The fact that our calculation favors the staggered geometry for the carbene complex **Ia** might be due to our fairly short $Cr-CH_2$ bond distance, which is 10−12 pm smaller than the M−E distances optimized by Nakatsuji and Fernández Sanz.

For the silylene complex **IIa**, we find the eclipsed structure to be the favored geometric arrangement. In the staggered conformation, we now have both a reduced steric repulsion and a reduced orbital interaction. As in the carbene case, it is not the difference in ΔE_{int}, but mainly the balance between ΔE^0 and ΔE_{prep}, which determines the more stable conformation. Our value for the rotational barrier E_{rot} = 0.5 kJ/mol compares well with the value obtained for $(CO)_5Cr{=}SiH(OH)$ (E_{rot}(SCF) = 0.46 kJ/mol).[23] The barrier reported for $(CO)_5Mo{=}SiH_2$ (E_{rot}(CASSCF) = 1.5 kJ/mol)[26] is somewhat higher than our result.

We further expect that the nature of the substituent R of the ER_2 ligand will significantly influence the rotational barrier. With increasing steric demand of the group R, the release in steric repulsion will dominate over the changes in the electronic interaction. Furthermore, the nature of the substituent R will influence the π interaction between the ER_2 group and the metal center and thus will affect the changes in ΔE_{int}. Essentially, our findings supoprt the notion of a basically free rotation around the M−E bond. The fine balance between steric repulsion and electronic interaction makes it difficult to establish a general rule whether an eclipsed or a staggered geometry is energetically favored.

Table 5. Optimized Bond Distances[a] and Bond Angles for $(CO)_5M{=}CH_2$ Complexes

	Ia: M = Cr	**Ib**: M = Mo	**Ic**: M = W	**Id**: M = Mn^+
d(M−C)	188.4	203.5	207.7	184.5
d(C−H)	110.7	110.7	110.6	110.3
∠(HCH)	109.9	109.1	109.4	110.7
$d(M-C)_{ax}$	189.2	208.7	214.0	187.6
$d(M-C)_{eq\parallel}$	185.4	202.7	207.2	182.7
$d(M-C)_{eq\perp}$	187.6	205.7	211.1	184.4
$d(C-O)_{ax}$	114.6	114.6	114.5	113.2
$d(C-O)_{eq\parallel}$	115.0	114.8	114.7	113.4
$d(C-O)_{eq\perp}$	114.5	114.4	114.3	113.2
$\angle(H_2C-MC_{eq\parallel})$	86.2	85.7	86.0	87.2
$\angle(H_2C-MC_{eq\perp})$	91.7	92.2	92.1	91.3

[a] Distances in pm and angles in deg.

Structures and Bonding of $(CO)_5M{=}CH_2$ (M = Cr, Mo, W) and $(CO)_5Mn{=}CH_2^+$. The optimized geometries for the eclipsed conformations of the complexes **Ia**, **Id**, **Ic** and **Id** are collected in Table 5. For a definition of the structural parameters, we once again refer to Figure 3. On going from chromium to tungsten, we observe a steady increase of the M=C bond length from 188.4 pm, **Ia**, to 203.5 pm, **Ib**, to 207.7 pm, **Ic**. The cationic manganese complex **Id**, which is isoelectronic to the complexes of the chromium triad, has a M=C distance of 184.5 pm. This is the shortest metal carbene bond length of the complexes investigated in this study. Similarly, we find an increase in the M−CO bond distances on going from the third row to the fifth row transition metals. For all complexes **Ia**−**Id**, the geometries of the carbene ligand and of the CO groups are very similar. Only the manganese complex possess C−O distances, which are about 1pm shorter compared to complexes **Ia**−**Ic**.

The bond analysis for complexes **Ia**−**Id** is presented in Table 6. For the tungsten compound, relativistic corrections were included in the energy calculation. It is interesting to note that for the chromium and the molybdenum compound the π bond strength $D_{\pi,\text{int}}$ is virtually identical: $D_{\pi,\text{int}}$ (**Ia**) = 202 kJ/mol and $D_{\pi,\text{int}}$ (**Ib**) = 204 kJ/mol. Further, it is the tungsten complex that possesses the highest π bond strength with $D_{\pi,\text{int}}$ (**Ic**) = 221 kJ/mol. The manganese compound **Id** has a π bond strength which is about 50 kJ/mol weaker than that of chromium. For $D'_{\sigma\text{int}}$, we calculate the following values: **Ia**, 154 kJ/mol; **Ib**, 132 kJ/mol; **Ic**, 180 kJ/mol; **Id**, 243 kJ/mol. The cationic complex **Id**, which has the lowest $D_{\pi,\text{int}}$ bond energy, now shows

(47) Holt, M. S.; Wilson, W. L.; Nelson, J. H. *Chem. Rev.* **1989**, *89*, 11.
(48) Brian, R. F. *J. Chem. Soc.* **1968**, 696.

Table 6. Bond Analysis[a] for $(CO)_5M{=}CH_2$ Complexes[a]

	ΔE^0	ΔE_{int}	$D_{\sigma,int}$	$D_{\pi,int}$	BE_{snap}	ΔE_{prep}	BE
Ia: M = Cr	113	−469	267	202	356	75	281
Ib: M = Mo	104	−440	236	204	336	82	254
Ic: M = W	53	−455	233	221	402	96	306
	(89)[b]	(−429)	(231)	(198)	(340)	(86)	(254)
Id: $M = Mn^+$	98	−493	341	152	395	76	319

[a] Energies are evaluated at the LDA/NL level of theory and are in kJ/mol. For the tungsten complex, quasi-relativistic corrections are included. [b] Nonrelativistic results in parentheses.

the largest value for $D'_{\sigma int}$. From Table 6, we find that for the neutral compounds the value for the intrinsic σ bond strength $D_{\sigma,int}$ decreases on going from chromium to tungsten. It is the remarkable drop in ΔE^0 which leads to the largest value of $D'_{\sigma,int}$ for the tungsten complex.

The exceptional bonding situation for **Id** is caused by the positive charge of the complex. Compared to those in the $Cr(CO)_5$ fragment, the frontier orbitals of $Mn(CO)_5^+$ are about 3 eV lower in energy. This stabilization is the consequence of an enhanced Coulomb attraction for the cationic complex **1d**. As a result, the LUMO of the metal fragment comes closer in energy to the HOMO of the CH_2 moiety, allowing for a better donation and a stronger σ bond interaction. Similary, the energy of the HOMO of the metal fragment is lowered, which in turn increases the energy gap between the orbitals involved in back donation and leads to a decrease of the π bond strength. Furthermore, the cationic complex serves as a more effective electron acceptor than its neutral counter parts, leading to an additional increase in $D_{\sigma,int}$.

The bonding in the tungsten complex **Ic** is significantly influenced by relativistic effects. In order to analyze these important contributions in more detail, we shall compare the results of a bond analysis without explicit treatment of relativistic effects to the results presented in Table 6.

The nonrelativistic steric interaction for $(CO)_5W{=}CH_2$ amounts to ΔE^0_{NR} = 89 kJ/mol, compared to the relativistic result of ΔE^0 53 kJ/mol. We see that relativistic effects reduce the steric interaction. This effect has been rationalized by Ziegler and co-workers.[29b,49a] The influence of the relativistic mass velocity term leads to a reduction in the electronic kinetic energy. This in turn will diminish the Pauli repulsion and thus will also decrease the value of ΔE^0.

The second important relativistic effect is an increase in the π-bond strength. The nonrelativistic W=C π bond strength amounts to $D_{\pi,NR}$ = 198 kJ/mol. This value again is close to that observed for **Ia** and **Ib**. Relativity stabilizes the W=C π-bond roughly by 20 kJ/mol. This effect can be rationalized by the relativistic destabilization of metal based d-orbitals.[49b,c] The relativistic core contraction leads to a more effective shielding of the nucleus.[49b,c] Thus, the valence d-orbitals are raised in energy. Consequently, orbitals of the tungsten pentacarbonyl fragment that carry a significant metal d-contribution, are also energetically destabilized. This effect is illustrated in Figure 6. The energy gap between the HOMO of the tungsten pentacarbonyl fragment and the LUMO of the carbene fragment is lowered, allowing for a more efficient π bond interaction. The slight destabilization of the σ bond is more than compensated by the before mentioned reduction of the steric repulsion.

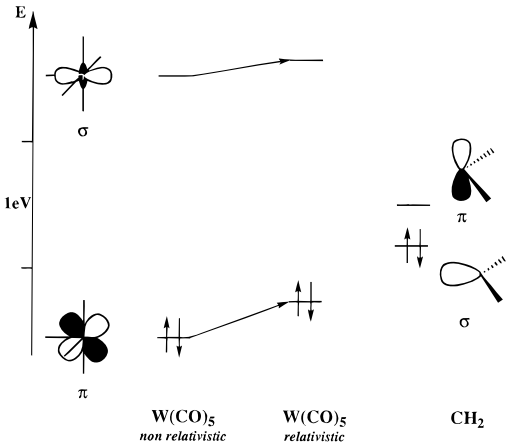

Figure 6. Effect of relativistic destabilization of the $(CO)_5W$ frontier orbitals. The HOMO of the metal fragment is raised in energy, allowing for a better bonding interaction with the empty ligand acceptor orbital.

We calculate the nonrelativistic W=C bond energy as $BE(W{=}C)_{NR}$ = 254 kJ/mol. This value is equal to that for the Mo complex and leads to the following ranking in bond strength: Cr > Mo = W. However, the introduction of relativistic effects significantly strengthens the W=C bond and results in the following order for the metal carbon double bond strength: W > Cr > Mo.

Comparison with Experimental Results. We conclude our discussion by comparing our calculated results with experimental values. We will begin with the geometric parameters. A general value for a Cr=C double bond in Fischer-type complexes lies between 200 and 204 pm for alkoxy carbenes, and between 209 and 216 pm for amino carbenes.[42] Compared to these values, our C=C bond length of 188.4 pm for **Ia** is significantly shorter. The same can be observed for the higher homologues of carbene complexes. Experimental values for the Cr=Ge[50] and the Cr=Sn[51] double bonds are 236.7 and 256.2 pm, respectively. The LDA geometries for complexes **IIIa** and **IVa** result in M=E distances that are 9−13 pm too short, compared with the experiment.

The calculated $M{=}CH_2$ distances are also too short for the heavier metals within the chromium triad. The two known Mo=C double bond lengths are 218[52] and 219.5 pm,[53] respectively. The carbon tungsten bond in $(CO)_5W{=}CPh_2$ has a representative bond length[54] of 215 pm. Whereas the LDA molybdenum carbon bond falls short by 12 pm (MO=C = 203.5 pm), the LDA tungsten−carbon bond distance comes within 7 pm to a closer agreement with the experiment. Again, we have to keep in mind that the experimental spectrum of W=C distances depends strongly on the nature of the carbene ligand with values ranging from 208.9 pm[55] in $(CO)_5W{=}CR(OMe)$-(R = cyclopent-3-enyl) to 222 pm[56] in $(CO)_5W{=}CR(OMe)$(R =3-cyclohexen-1-yl).

One can provide several explanations to account for the short M=E bond lengths. It has been shown that LDA geometries

(49) (a) Ziegler, T.; Snijders, G. J.; Baerends, E. J. In *The Challenge of d and f Electrons*; Salahub, D. R., Zerner, M. C., Eds.; ACS Symposium Series 395; American Chemical Society: Washington, DC, 1989; p 322. (b) Pyykkö, P.; Declaux, J.-P. *Acc. Chem. Rev.* **1979**, *12*, 276. (c) Pyykkö, P. *Chem. Rev.* **1988**, *88*, 563.

(50) Jutzi, P.; Steiner, W.; König, E.; Huttner, G.; Frank, A.; Schubert, U. *Chem. Ber.* **1978**, *111*, 606.

(51) Cotton, J. D.; Davidson, P. J.; Lappert, M. F. *J. Chem. Soc., Dalton Trans.* **1976**, 2275.

(52) Dai, X.; Li, G.; Chen, Z.; Tang, Y.; Chen, J.; Lei, G.; Xu, W. *Jiegou Huaxue* **1988**, *7*, 22.

(53) Erker, G.; Dorf, U.; Krüger, C.; Tsay, Y.-H. *Organometallics* **1987**, *6*, 680.

(54) Casey, C. P.; Burkhardt, T. J.; Bunnell, C. A.; Calabrese, J. C. *J. Am. Chem. Soc.* **1977**, *99*, 2127.

(55) Toledano, C. A.; Parlier, A.; Rudler, H.; Daran, J.-C.; Jeannin, Y. *J. Chem. Soc., Chem. Commun.* **1984**, 576.

(56) Alvarez, C.; Pacreau, A.; Parlier, A.; Rudler, H.; Daran, J.-C. *Organometallics* **1987**, *6*, 1057.

for transition metal complexes underestimate the metal−ligand distance by 4−6 pm.[57] Further, we have to ask the question how well our model compound describes the experimentally known structures. From the variety of known chromium and tungsten carbenes, one can see that the M═C bond length is highly depended on the nature of the carbene substituents, and can vary over a range of 16 pm. One factor is the steric bulk provided by the substituents R^1, R^2 of carbene ligands CR^1R^2. Increasing steric hinderance between the R^1, R^2 groups and the metal fragment will lead to an elongation of the M═C bond length. We further have to keep in mind that the experimentally known carbene complexes are formed with carbene ligands that possess a singlet ground state, which also resembles the electronic valence state. As a consequence, the LUMO acceptor orbital for $^1CR^1R^2$ ligands will be higher in energy than that of $^1CH_2$*. Thus, the M═C bond strength is reduced due to a weaker π component of the bond. We can therefore expect that M═C in methylene complexes should be shorter than that in carbene CR^1R^2 complexes, where the CR^1R^2 ligand has a singlet ground state and sterically demanding substituents.

For coordinatively saturated molecules, the experimentally available metal-carbene bond dissociation enthalpies are limited to three $Mn(CO)_5CXY$ molecules: $D[Mn(CO)_5^+{=}CH_2] = 401 \pm 31$ kJ/mol, $D[Mn(CO)_5^+{=}CHF] = 356 \pm 25$ kJ/mol, and $D[Mn(CO)_5^+{=}CF_2] = 332 \pm 12$ kJ/mol. Each one of these results was obtained by photoionization mass spectrometry.[58] Our calculated bond energy for $(CO)_5Mn{=}CH_2^+$, **Id**, amounts to BE(**Id**) = 319 kJ/mol. This value is 82 kJ/mol too small compared to the experimental result. One crucial factor for the theoretical bonding energy is the contribution from the preparation energy. The singlet−triplet splitting energy for methylene $\Delta E_{ST}(CH_2)$ still provides a challenge to density functional theory, and the LDA/NL calculation overestimates $\Delta E_{ST}(CH_2)$ by 27 kJ/mol.[41] If we correct our bond snapping energy for **Id** with the experimental value[21] of 38 kJ/mol for $\Delta E_{ST}(CH_2)$, we obtain an improved bonding energy of BE(**Id**) = 346 kJ/mol, in closer agreement to the experiment. Despite the large experimental error margin, there still remains a discrepancy between the theoretical and experimental value for $D[Mn(CO)_5^+{=}CH_2]$.

Accurate experimental $M{=}CR_2$ bonding energies for a series of homologous Fischer carbenes within the chromium triad are not available. However, it has been observed[59] that chromium carbenes are less stable than similar tungsten derivatives but more stable than analogous molybdenum compounds. This observed stability ranking W > Cr > Mo is in accord to the calculated trend for M═C bond strengths.

4. Conclusion

In the present DFT study, we investigated geometries and bonding in Fischer-type compounds. One of the goals was to examine how the bonding between transition metal carbenes varies from that in transition metal silylenes and higher homologues. The remarkable difference is the drop in the intrinsic π bond strength: The π bond between CH_2 and the chromium fragment $Cr(CO)_5$ is more than twice as strong as that for the SiH_2 moiety. The π contributions for SiH_2, GeH_2, and SnH_2 are comparable. This difference in π bond strength manifests itself in geometric parameters of the transition metal complexes, as for example the bond length between the metal center and the axial CO ligand. We explained the difference in π bonding by comparing the electronic valence states of the main group fragments. The weak π bond in turn is also responsible for the differences of coordination as well as the reaction chemistry between carbene complexes and their higher homologues.

If we compare the bonding between CH_2 and metal pentacarbonyl fragments within the chromium triad, we find that the W═C bond is noticeably stabilized by relativistic effects. The relative bond strengths can be arranged in the following order: W > Cr > Mo.

It remains to investigate how a variation of the ER_2 ligand influences the Cr═E bond strength as well as the geometry of the carbene complex. Further, it is of interest to elucidate the influence of nonlocal corrections as well as relativistic contributions on the geometry of transition metal carbenes. We will address both problems in forthcoming studies.[60]

Acknowledgment. This investigation was supported by the Natural Science and Engineering Research Council of Canada (NSERC), and by the donors of the Petroleum Research Fund, administered by the American Chemical Society (ACS-PRF No. 27023-AC3).

IC941006Q

(57) (a) Fan, L.; Ziegler, T. *J. Chem. Phys.* **1991**, *95*, 7401. (b) Fan, L. Ph.D. Thesis University of Calgary, 1992.
(58) Stevens, A. E. Ph.D. Thesis, California Institute of Technology, 1981.
(59) Kirtley, S. W. In *Comprehensive Organometallic Chemistry*, 1st ed.; Wilkinson, G., Stone, F. G. A., Abel, E. W., Eds.; Pergamon Press: Oxford, England, 1982; Vol. III, p 899.
(60) (a) Jacobsen, H.; Ziegler, T. *Organometallics* **1995**, *14*, 224. (b) Jacobsen, H.; Schreckenbach, G.; Ziegler, T. *J. Phys. Chem.* **1994**, *98*, 11406.